

# Direct Optical Excitation of Quantum-Degenerate Exciton States in Semiconductors

M. Kira and S.W. Koch

*Department of Physics and Material Sciences Center,  
Philipps-University Marburg, Renthof 5, D-35032 Marburg, Germany*

G. Khitrova and H.M. Gibbs

*Optical Sciences Center, University of Arizona, Tucson, AZ 85721, USA*

(Dated: November 23, 2018)

Quantum electrodynamic calculations predict that truly incoherent light can be used to efficiently generate quantum-degenerate exciton population states. Resonant incoherent excitation directly converts photons into excitons with vanishing center of mass momentum. The populated exciton state possesses long-range order, is very stable against perturbations, and should be observable via its unusual directional and density dependence in luminescence measurements.

PACS numbers: 71.35.Lk, 03.75.Kk, 78.55.-m

Parallel to atomic Bose-Einstein condensation studies[1], semiconductor researchers are on an elusive and persistent quest[2, 3, 4, 5, 6, 7, 8, 9, 10] to achieve macroscopic populations of quantum-degenerate exciton states and Bosonic condensation. However, such attempts encounter several serious obstacles in GaAs-like direct band-gap systems since the elementary electron-hole pair excitations have a relatively short life time in the nanosecond range. Especially, photoluminescence recombines very efficiently electron-hole pairs, and in particular low-momentum excitons, on a time scale of some tens of picoseconds, which leaves a strong hole-burning signature in the exciton center-of-mass momentum distributions.[11] As a result, simple thermodynamic Bose-Einstein condensation is difficult to realize even for conditions where the large majority of electron-hole pairs exists in the form of excitons. Thus, coupling to incoherent fields clearly seems to be a highly undesirable aspect for excitonic condensation since radiative exciton recombination opposes the macroscopic accumulation into the lowest energy and momentum state. Consequently, most of the recent exciton-condensation experiments have either concentrated on  $\text{Cu}_2\text{O}$ [5, 6] where the energetically lowest exciton state is dipole forbidden, or on indirect semiconductor systems [7, 8, 9, 10] with strongly suppressed radiative coupling.

In this context, it is an interesting question to ask whether one can completely change the negative influence of incoherent fields on condensation into a virtue *by using truly incoherent excitation pulses to pump — not to drain — direct band-gap systems*. To answer this question, we show in this Letter that by using quantum fields with finite intensity but vanishing phase, one can devise an incoherent optical excitation scheme which selectively generates a very discrete set of low-momentum exciton states. This pumping directly seeds a many-body state with an exciton population that exhibits long-range order. We show that this state is remarkably stable against

Coulomb and phonon scattering and should be directly observable experimentally via its directional emission and its unusual dependence on excitation strength. Furthermore, we discuss how additional amounts of coherent excitation modify the generation process.

We investigate situations where a direct band-gap semiconductor is resonantly excited either with a fully or partially incoherent electromagnetic field. In our quantum-electrodynamic approach we treat the light field via bosonic photon operators  $B_{\mathbf{q},q_\perp}$  and  $B_{\mathbf{q},q_\perp}^\dagger$  related to a plane-wave mode with momentum  $(\mathbf{q}, q_\perp)$ , where  $\mathbf{q}$  and  $q_\perp$  are the in-plane and perpendicular momentum components, respectively. The semiconductor is assumed to be a two-band quantum-well or quantum-wire system, described by fermionic operators  $a_{c(v)}$ , and  $a_{c(v)}^\dagger$ , related to destruction and generation of conduction (valence) band electrons with in-plane momentum  $\mathbf{k}$ . We include the microscopic Coulomb interaction together with coupling of carriers to photons and phonons. The equations of motion for the interacting photon-carrier-phonon system lead to the well-known hierarchy problem[12]. We use the cluster-expansion scheme[13] at a level where all two-particle correlations are fully included while the three-particle correlations are treated at the scattering level. As a result, the coherent part of the excitation is described by the well-known Maxwell-semiconductor Bloch equations [12] including two-particle Coulomb and phonon scattering.[14]

The most important novel aspect of the present studies is the modeling of the incoherent pumping which, in contrast to coherent optical excitation, does not induce an interband polarization, but generates photon-assisted polarizations  $\Delta\langle Ba_c^\dagger a_v \rangle$  ( $\Delta\langle B^\dagger a_v^\dagger a_c \rangle$ ) describing correlated absorption (emission) of a photon while an electron-hole pair is generated (recombined). These assisted polarizations then act as sources for the generation of electron  $f_{\mathbf{k}}^e \equiv \langle a_{c,\mathbf{k}}^\dagger a_{c,\mathbf{k}} \rangle$  and hole distributions  $f_{\mathbf{k}}^h \equiv \langle a_{v,\mathbf{k}} a_{v,\mathbf{k}}^\dagger \rangle$  as well as exciton correlations

$c_X^{\mathbf{q},\mathbf{k}',\mathbf{k}} \equiv \Delta\langle a_{c,\mathbf{k}}^\dagger a_{v,\mathbf{k}'}^\dagger a_{c,\mathbf{k}'+\mathbf{q}} a_{v,\mathbf{k}-\mathbf{q}} \rangle$  which are obtained from the two-particle expectation values by removing the single-particle contributions.

From the semiconductor luminescence equations [15], we see that the source terms for the photon-assisted polarizations are

$$\begin{aligned} \frac{\partial}{\partial t} \Delta\langle B_{\mathbf{q},q_\perp}^\dagger a_{v,\mathbf{k}-\mathbf{q}}^\dagger a_{c,\mathbf{k}} \rangle|_{\text{source}} &= \mathcal{F}_q [f_{\mathbf{k}}^e f_{\mathbf{k}-\mathbf{q}}^h + \sum_{\mathbf{n}} c_X^{\mathbf{q},\mathbf{k},\mathbf{n}} \\ &+ (f_{\mathbf{k}}^e + f_{\mathbf{k}-\mathbf{q}}^h - 1) \Delta\langle B_{\mathbf{q},q_\perp}^\dagger B_{\mathbf{q}\Sigma} \rangle]. \end{aligned} \quad (1)$$

The self-consistent propagation of the incoherent light field is computed from

$$\begin{aligned} \frac{\partial}{\partial t} \Delta\langle B_{\mathbf{q},q_\perp}^\dagger B_{\mathbf{q},q'_\perp} \rangle &= i(\omega_q - \omega_{q'}) \Delta\langle B_{\mathbf{q},q_\perp}^\dagger B_{\mathbf{q},q'_\perp} \rangle \\ &+ \mathcal{F}_q \sum_{\mathbf{k}} \Delta\langle B_{\mathbf{q},q'_\perp}^\dagger a_{c,\mathbf{k}}^\dagger a_{v,\mathbf{k}-\mathbf{q}} \rangle \\ &+ \mathcal{F}_{q'}^* \sum_{\mathbf{k}} \Delta\langle B_{\mathbf{q},q_\perp}^\dagger a_{v,\mathbf{k}-\mathbf{q}}^\dagger a_{c,\mathbf{k}} \rangle, \end{aligned} \quad (2)$$

where  $\mathcal{F}_q \equiv d_{vc} \mathcal{E}_{\mathbf{q},q_\perp} u_{\mathbf{q},q_\perp} / \hbar$ ,  $d_{vc}$  is the dipole-matrix element of the direct band-gap semiconductor,  $\mathcal{E}_q$  is the vacuum-field amplitude, and  $u_q$  is the mode strength at the quantum well or wire position. Furthermore, we introduced the operator  $B_{\mathbf{q}\Sigma} \equiv \sum_{q_\perp} d_{vc} \mathcal{E}_{\mathbf{q},q_\perp} u_{\mathbf{q},q_\perp} B_{\mathbf{q},q_\perp}$  which gives the total photon operator with momentum component  $\mathbf{q}$  along the confined system. Equation (1) shows that the photon-assisted polarization can be generated either via the stimulated term  $\Delta\langle B^\dagger B \rangle$  or via the spontaneous term including the electron-hole plasma source ( $f^e f^h$ ) as well as the exciton-correlation contribution.

The incoherent source terms for the carrier distributions and the excitonic correlations are

$$\hbar \frac{\partial}{\partial t} f_{\mathbf{k}}^e|_{\text{inc}} = -2\text{Re} \left[ \sum_{\mathbf{q}} \Delta\langle B_{\mathbf{q}\Sigma}^\dagger a_{v,\mathbf{k}-\mathbf{q}}^\dagger a_{c,\mathbf{k}} \rangle \right], \quad (3)$$

$$\frac{\partial}{\partial t} f_{\mathbf{k}}^h|_{\text{inc}} = -2\text{Re} \left[ \sum_{\mathbf{q}} \Delta\langle B_{\mathbf{q}\Sigma}^\dagger a_{v,\mathbf{k}}^\dagger a_{c,\mathbf{k}+\mathbf{q}} \rangle \right], \quad (4)$$

$$\begin{aligned} \hbar \frac{\partial}{\partial t} c_X^{\mathbf{q},\mathbf{k}',\mathbf{k}}|_{\text{inc}} &= (f_{\mathbf{k}}^e + f_{\mathbf{k}-\mathbf{q}}^h - 1) \Delta\langle B_{\mathbf{q}\Sigma}^\dagger a_{v,\mathbf{k}'}^\dagger a_{c,\mathbf{k}'+\mathbf{q}} \rangle \\ &+ (f_{\mathbf{k}'+\mathbf{q}}^e - f_{\mathbf{k}'}^h - 1) \Delta\langle B_{\mathbf{q}\Sigma} a_{c,\mathbf{k}}^\dagger a_{v,\mathbf{k}-\mathbf{q}} \rangle. \end{aligned} \quad (5)$$

The full equation for  $\frac{\partial}{\partial t} c_X^{\mathbf{q},\mathbf{k}',\mathbf{k}}$  contains additionally the Coulomb and phonon terms responsible for the formation of exciton populations including the true fermionic substructure.[11, 16, 17]

Since the  $\mathbf{q}$  component of the photon is very small compared to any typical carrier momentum, the exciton correlations couple to the incoherent light field only when their center-of-mass momentum  $\mathbf{q}$  is nearly vanishing. Experimentally, the in-plane photon momentum  $\mathbf{q}$  can be fixed by controlling the excitation direction which,

e.g., for normal incidence leads to the exclusive population of the zero momentum exciton state. Similar selectivity clearly does not exist for the carrier densities.

In our numerical evaluations, we assume pulsed incoherent excitation by choosing the initial condition according to

$$\Delta\langle B_{\mathbf{q},q_\perp}^\dagger B_{\mathbf{q},q'_\perp} \rangle|_{t=0} = \Delta I_{\mathbf{q}} e^{-[(q_\perp - q_0)^2 + (q'_\perp - q_0)^2] / \Delta q^2}, \quad (6)$$

containing  $\Delta I_{\mathbf{q}}$  which determines the incoherent intensity in a given direction. The central frequency of the incoherent excitation is  $\omega_0 = cq_0$  while its energy and temporal width is determined by  $\Delta q$ . Solving our coupled equations with only this incoherent excitation source, we verify that no semiclassical optical polarization is generated, however, the photon-assisted polarization builds up via the stimulated term in Eq. (1). This then leads to the generation of carrier distributions in a wide range of momentum states but exciton correlations are generated only in the low-momentum states defined by  $\Delta I_{\mathbf{q}}$ .

To illustrate the main effects of resonant excitation with truly incoherent light, we numerically solve the full set of equations (1)-(5) including the semiconductor luminescence and Bloch equations with the microscopic Coulomb and phonon scattering included. As an example, we investigate the case of a quantum-wire system with typical GaAs material parameters providing 11 meV exciton binding energy and a 3D-Bohr-radius of  $a_0 = 12.5$  nm. We study low-temperature, resonant excitation configurations such that only acoustic phonons need to be included. The combined treatment of the semiconductor luminescence and Maxwell-semiconductor Bloch equations allows us to freely alter the coherence level of the excitation pulses since we can adjust the relative intensities of the incoherent and coherent parts. The generated many-body state after each excitation condition can be followed by computing exciton distributions  $\Delta n_{\lambda}(\mathbf{q}) \equiv \sum_{\mathbf{k},\mathbf{k}'} \phi_{\nu}^*(\mathbf{k}) \phi_{\nu}(\mathbf{k}) c_X^{\mathbf{q},\mathbf{k}'-\mathbf{q},\mathbf{k}+\mathbf{q}}$  including the exciton wave functions  $\phi_{\nu}(\mathbf{k})$  [17]. Spatial correlations and long-range order effects are determined from the correlation function between two electron-hole pairs,

$$g_{\text{ord}}(\mathbf{r}) \equiv \Delta\langle P^\dagger(0)P(\mathbf{r}) \rangle = \frac{1}{\mathcal{V}^2} \sum_{\mathbf{q},\mathbf{k}',\mathbf{k}} c_X^{\mathbf{k},\mathbf{k}',\mathbf{q}} e^{i\mathbf{q}\cdot\mathbf{r}}, \quad (7)$$

which involves creation  $P^\dagger(\mathbf{r})$  and annihilation  $P(\mathbf{0})$  of an electron-hole pair at different positions while  $\mathcal{V}$  is the quantization volume.

For excitation at the 1s exciton resonance, we show in Fig. 1 a comparison of the generated incoherent exciton density  $\Delta n_{1s} = \frac{1}{\mathcal{V}} \sum_{\mathbf{q}} \Delta n_{1s}(\mathbf{q})$  (thick solid and dashed lines) and the corresponding exciton density at the lowest momentum states (thin solid and dashed lines) for both completely coherent (dashed line) and completely incoherent (solid line) excitation pulses of the same intensity (dark shaded area). Even though both excitations give

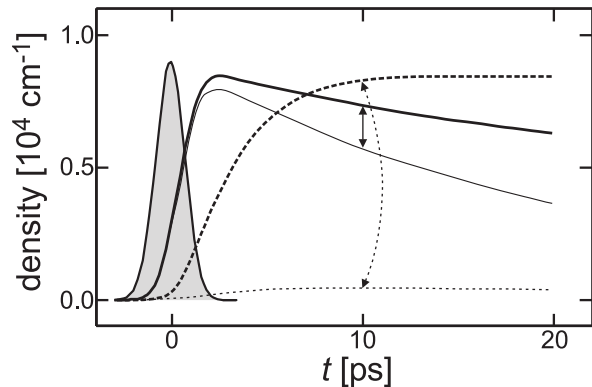


FIG. 1: Generation of excitons with completely incoherent (solid lines) or coherent excitation (dashed lines) pulses for a temperature of  $4K$ . The temporal evolution of the excitation pulse (shaded area), the generated  $1s$ -exciton density (thick lines), and the density in the lowest momentum states (thin lines) are shown. The arrows denote curves belonging to the same excitation conditions.

rise to well-above 90% exciton fractions with respect to the total carrier density  $\frac{1}{V} \sum_{\mathbf{k}} f_{\mathbf{k}}^{e(h)}$ , the coherent and incoherent excitations are characterized by very different dynamics and final exciton states. For the coherent case, the excitation first generates optical polarization which gradually is converted into incoherent exciton populations [14]. However, less than 5% of these excitons are found in the low-momentum states (thin dashed line). In contrast, for completely incoherent excitation, the direct conversion of photons into excitons leads to an almost instantaneous build-up of a low-momentum exciton population (solid line). The generation of such a state is followed by radiative recombination of low-momentum excitons.

In order to gain more insight into the incoherent excitation process, we compare the generated exciton distributions for coherent and incoherent excitation conditions. For this purpose, we determine  $\Delta n_{1s}(\mathbf{q})$  at a time moment when the generation process has been completed (indicated by arrows in Fig. 1). Figure 2a shows the incoherently (shaded area) and coherently (dashed line) generated  $\Delta n_{1s}(\mathbf{q})$  determined at 10 ps after the pulse maximum for a lattice temperature  $T = 4K$ . We observe that the coherently generated populations have a broad momentum distribution, whereas the incoherent excitation leads to a highly singular  $1s$ -exciton distribution around the zero-momentum state. This distribution is remarkably stable against carrier and phonon scattering (see inset to Fig. 2a). In Fig. 2b we plot the corresponding pair-correlation functions showing that for the coherently generated state the pair-correlation function  $g_{\text{ord}}(\mathbf{r})$  (dashed line) decays on the length scale of the 3D-Bohr radius  $a_0$ , whereas the incoherent  $g_{\text{ord}}(\mathbf{r})$  (shaded area) exhibits pronounced long-range order. The observation of the singular  $1s$ -exciton distributions and the existence

of long-range order uniquely demonstrate that incoherent pumping directly produces a highly quantum-degenerate exciton state.

Now we turn to the questions concerning the robustness of the incoherently generated exciton state and how to observe it in experiments. In Fig. 3a, we plot the exciton population for different intensities of the incoherent field showing that the macroscopic population of the  $1s$  state continuously increases up to the intensity level  $\Delta I = 10$ , which corresponds to a generated carrier density of  $na_0 = 0.1$ . For this situation, basically all of the excitons are in the low-momentum state. For higher excitation levels, the  $1s$ -exciton population starts to decrease because the underlying fermion character of the electron-hole pairs gradually prevents further exciton accumulation. The quantum-degenerate state ceases to exist above  $\Delta I = 31$  corresponding to a density  $n_e a_0 = 0.3$ . In our studies of lattice temperature effects, we find that the results presented here are valid for temperatures of less than approximately  $6 - 10K$ . For higher temperatures, acoustic phonon scattering gradually leads to population scattering into higher momentum states (see inset to Fig. 2a).

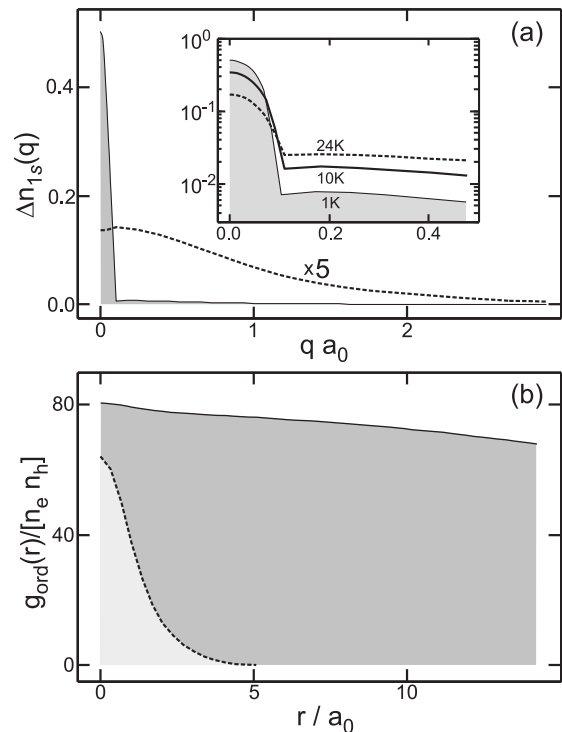


FIG. 2: (a) Exciton distributions resulting from coherent (dashed line, curve multiplied by 5) and incoherent (shaded area) pumping for a lattice temperature  $T = 4K$  of Fig. 1 at time indicated by arrows. The inset shows the incoherently generated distributions at lattice temperatures of  $1K$  (shaded area),  $10K$  (solid line), and  $24K$  (dashed line). (b) The corresponding pair-correlation functions determined from Eq. (7).

Since we investigate the case of direct-gap semiconduc-

tors, the macroscopic 1s-exciton population recombines at the rate of the radiative decay time. The corresponding photoluminescence is emitted with the same in-plane momentum as the condensate. As a result, the presence of a macroscopic population at  $\mathbf{q} = \mathbf{0}$  should show up as a strong directional dependence of the luminescence.[18]

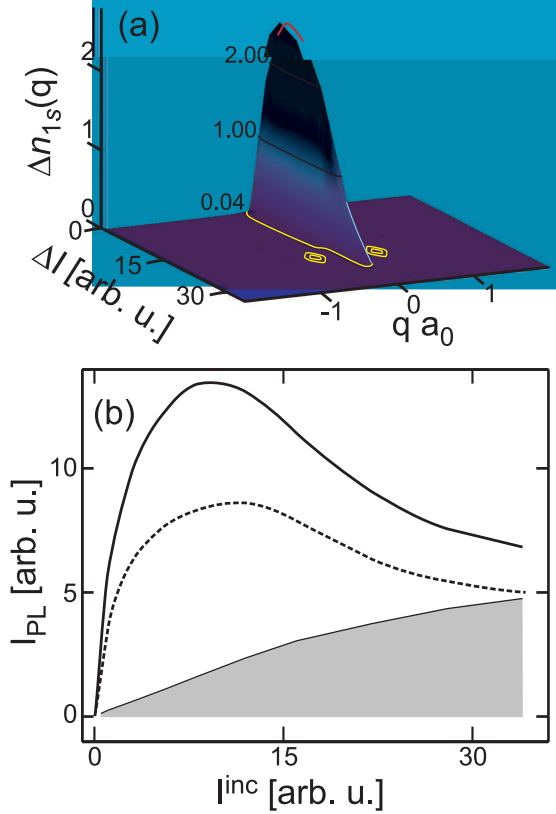


FIG. 3: (a) Exciton distributions as function of intensity of incoherent field determined 16 ps after the excitation for the 100% incoherent excitation at  $T = 4K$ . (b) Total photoluminescence resulting from 100%coherent (shaded area), 40%coherent (dashed line), and 100%incoherent (solid line) pumping determined 16 ps after the excitation.

Additionally, the intensity dependence of the population in Fig. 3a manifests itself as an unusual intensity dependence of the integrated photoluminescence,  $I_{PL} = \sum_{\mathbf{q}} \frac{\partial}{\partial t} \Delta(B_{\mathbf{q}}^\dagger B_{\mathbf{q}})$ . As an example, we show in Fig. 3b the variation of  $I_{PL}$  as function of pump intensity determined 16 ps after 100% incoherent (solid line), 40% coherent (dashed line), and 100% coherent (shaded area) excitation. We see that for the relatively low levels of excitation studied here, the total luminescence for the 100% coherent case exhibits the expected practically linear dependence on the excitation strength. However, when we include a significant incoherent component to the excitation process,  $I_{PL}$  behaves strongly nonmonotonously. For 100% incoherent excitation, the luminescence is maximized at the intensity level  $\Delta I = 10$  corresponding to the maximum singularity of exciton distributions in Fig. 3a.

Since the zero momentum state population decreases for elevated intensities, the luminescence decreases also until it reaches the same level as that for coherent excitation. This predicted distinct nonmonotonic behavior of  $I_{PL}$  should be directly observable in experiments serving as a clear signature for the formation of the quantum-degenerate exciton state. We note in Fig. 3b, that  $I_{PL}$  has a maximum even in the presence of 40% coherent excitation, indicating that a significant population in the quantum-degenerate state is generated even in this imperfect case.

In summary, our microscopic calculations lead us to predict that resonant incoherent excitation with fields of finite intensity but vanishing phase directly generates a macroscopic population of 1s-excitons in low-momentum states. This quantum-degenerate state possesses significant long range order and is remarkably stable against perturbations. As predicted experimental signatures, the integrated luminescence displays distinct non monotonic behavior since it first increases and then decreases with increasing excitation intensity.

The Marburg work is funded by the Optodynamics Center and the Deutsche Forschungsgemeinschaft through the Quantum optics in semiconductors research group. The Tucson work is funded by NSF AMOP.

- 
- [1] E.A. Cornell and C.E. Wieman, Rev. Mod. Phys. **74**, 875 (2002); W. Ketterle, Rev. Mod. Phys. **74**, 1131 (2002).
  - [2] M. Girardeau and R. Arnowitt, Phys. Rev. **113**, 755 (1959).
  - [3] E. Hanamura and H. Haug, Phys. Lett. **33**, 209 (1977).
  - [4] L.L. Chase, N. Peyghambarian, G. Grynberg, and A. Mysyrowicz, Phys. Rev. Lett. **42**, 1231 (1979).
  - [5] D. Snoke, J.P. Wolfe, and A. Mysyrowicz, Phys. Rev. Lett. **59**, 827 (1987).
  - [6] J.L. Lin and J.P. Wolfe, Phys. Rev. Lett. **71**, 1222 (1993).
  - [7] L.V. Butov, A. Zrenner, G. Abstreiter, G. Bohm, and G. Weimann, Phys. Rev. Lett. **73**, 304 (1994).
  - [8] L.V. Butov, A.C. Gossard, and D.S. Chemla, Nature **418**, 751 (2002).
  - [9] D. Snoke, S. Denev, Y. Liu, L. Pfeiffer, and K. West, Nature **418**, 754 (2002).
  - [10] R. Rapaport et al., Phys. Rev. Lett. **92**, 117405 (2004).
  - [11] M. Kira, W. Hoyer, T. Stroucken, and S.W. Koch, Phys. Rev. Lett. **87**, 176401 (2001);
  - [12] H. Haug and S.W. Koch, *Quantum Theory of the Optical and Electronic Properties of Semiconductors* (World Scientific Publ., Singapore, 4th ed., 2004).
  - [13] H.W. Wyld and B.D. Fried, Ann. Phys. **23**, 374 (1963); J. Fricke, Ann. Phys. **252**, 479 (1996); M. Kira *et al.*, J. Nonlin. Opt. B **29**, 481 (2002).
  - [14] M. Kira and S. W. Koch, Phys. Rev. Lett. **93**, 076402 (2004).
  - [15] M. Kira, W. Hoyer, F. Jahnke, and S. W. Koch, Prog. Quantum Electron. **23**, 189 (1999).
  - [16] T. Usui, Prog. Theor. Phys. **23**, 787 (1960).
  - [17] W. Hoyer, M. Kira, and S.W. Koch, Phys. Rev. B **67**,

- 155113 (2003)
- [18] J. Keeling, L.S. Levitov, and P.B. Littlewood, Phys. Rev. Lett. **92**, 176402 (2004).